PREDICTION OF STRONG MOTIONS FROM FUTURE EARTHQUAKES CAUSED BY ACTIVE FAULTS – CASE OF THE OSAKA BASIN

Kojiro IRIKURA[1]

SUMMARY

A methodology is proposed for estimating strong ground motions from scenario earthquakes caused by active faults. We summarize the procedure that is currently used to characterize earthquake rupture models for the prediction of ground motions, based on geological investigations of capable earthquake faults and seismological studies of source models. Total fault lengths of scenario earthquake would be evaluated from survey of segmentation and grouping of active faults for a long-term prediction of seismic activity. The fault widths are evaluated based on the thickness of seismogenic zones from the cut-off depth of small earthquakes. The seismic moment of the capable faults are estimated by the empirical relationship between the source areas and seismic source, then average slips are automatically constraint from the seismic moment and source area. The scaling relations of modeling slip heterogeneity constructed based on a statistical analysis of the source inversion of crustal earthquakes ranging from about 6 to 7 in moment magnitude(Mw) (Somerville et al.,1999). We use a set of parameters to quantify in a deterministic manner the distribution of asperities satisfying the heterogeneity of slip on the fault surface and its two-dimensional Fourier transform of the k-squared model by Herrero and Barnard(1994). The procedure proposed here is applied for estimating strong ground motions from hypothetical large earthquakes in the Osaka metropolitan area.

INTRODUCTION

Scenario earthquake for subject areas has gradually been popular to make a seismic disaster prevention measure by some governmental agencies and municipalities in Japan. However, most of strong motion estimation in earthquake hazard analysis are still inclined to empirical methods. Peak ground acceleration and velocity and response spectrum for earthquake-resistant design are given by the empirical methods as a function of magnitude, fault distance, ground condition. They have not reflected yet recent results of rapidly progressing researches in seismology, such as rupture theory of source processe in earthquake faults and simulation techniques of wave propagation in irregular sedimentary layers. Concentration of damages in particular areas such as “damage belt” during the 1995 Hyogo-ken Nanbu Earthquake cannot explained without considering earthquake source and actual geological configurations.

We attempted to make a recipe to popularize the prediction of ground motions for engineering purpose based on seismological fruits. There are two important factors, one is estimation of the Green’s functions from source to site, the other is source characterization based on geological features for active faults and statistical analysis of source processes for waveform inversion of strong motion records. For the former we adopt a hybrid method estimating Green's functions, deterministic and stochastic approaches in low (< 1 Hz) and high (> 1 Hz) frequency ranges, respectively, to obtain broad-band ground motions. For latter, we summerize global and local source parameters for estimating ground motions. The global parameters such as total fault length, width, seismic moment and so on are obtained based on geological investigations of capable earthquake faults and seismological studies of source models. The local source parameters are slip heterogeneity on fault plane from a statistical analysis of the source inversion of crustal earthquakes. Source modeling is given on self-similar

[1] *Disaster Prevention Research Institute, Kyoto University, Kyoto, Japan E-mail: irikura@egmdpri01.dpri.kyoto-u.ac.jp*

scaling relations of asperities satisfying the heterogeneity of slip on the fault surface and its two-dimensional Fourier transform of the k-squared model.

We have attempted to make seismic hazard analysis in Osaka, estimating strong ground motions from hypothetical earthquakes beneath and near urbanized areas. We select active faults that have high possibilities of causing large earthquakes in near future, survey the geological configuration around the faults, estimate amplifications in the target areas due to the propagation-path and site theoretically and semi-empirically, and make strong motion prediction with the highest reliability that is possible at the current standard of technology.

RECIPE OF STRONG MOTION PREDICTION

We have successfully developed the empirical Green's function method to estimate strong ground motion for large earthquakes using observed records from small events occurring near the source area of the large event (Irikura, 1986). The small event records are superimposed to follow the scaling relations of the source dynamics. In this method broadband ground motions of engineering interest are estimated without calculating the Green's functions in complicated and realistic media. However, there are two problems to apply this method. One is that this method is only applicable as long as we have appropriate records usable as the Green's functions. In many cases we have no records, then cannot use this method. Then we propose hybrid methods for estimating broadband ground motions in **2.1**. The other is the source characteristics. The scaling law of earthquakes show only average source characteristics. To calculate ground motions near faults, we need to know heterogeneous slip and slip velocity distribution in the rupture areas for large earthquakes more than 6.5. The latter problem is solved in **2.2** as the asperity source model.

Hybrid Method for Estimating Ground Motions

In case of no appropriate records from small events we use hybrid schemes, deterministic at low frequencies and stochastic at high frequencies. One is the hybrid Green's function method in which broad-band motions from small-events are calculated, (Kamae et al. 1998). For low frequency motion less than 1 Hz, we calculate small event records considering a double couple point source in the 3-D structure from source to site using a 3-D finite difference method (Pitarka and Irikura, 1996). For high frequency motion more than 1 Hz, we simulate ground motion from the small event with the same size as the lower frequency motion using the stochastic method by Boore(1983). The numerical Green's functions are obtained summing such low and high frequency motions in the flow as shown in Fig. 1. Then we compute strong ground motion from large earthquakes for the target source areas using the simulated small event motions as the empirical Green's functions following the asperity source model with heterogeneous slip distributions as discussed later.

The other is the hybrid simulation method (Irikura and Kamae, 1999). In a near-fault area, ground motions are strong affected by radiation pattern effects due to source type. Then to simulate accurate ground motions we need to calculate a number of the numerical Green's functions. In that case the long period motions from the large earthquake are directly simulated with the 3-D Finite Difference Method taking into account the asperity source model and the 3-D structure. The short period motions are calculated following almost the same idea as the hybrid Green's function methd because the radiation pattern effects are smoothed in the short-period range.

Source Characterization

Another important issue for strong motion prediction is source process for a future earthquake. We take into account earthquakes caused by active faults. A question is "Do earthquakes due to specific active fault have repeatedly similar source process ?". If yes, it is possible to make source modeling for future earthquakes. One answer would be obtained follows from geological and geographical investigations so far done. Long-term evaluation of earthquakes have been made based extensive research of segmentation and grouping of active faults. They found that slip distributions along fault segments have similar features to the results from the source inversion using seismic data, e. g. slip is largest in the middle of the segment and decreases towards the edge as shown in Fig. 2. The other possible answer would be fault dynamics estimated by the waveform inversion of strong motion records. Bouchon et al. (1998) studied the characteristics of stress field before and after the 1995 Hyogoken Nanbu earthquake based on the results of the source inversion using near-field recordings. There is a relatively strong correlation between the initial and final stress distribution, which suggests that intrinsic fault properties, not modified by the earthquake, control the spatial distribution of tectonic stress over fault. Those results suggest the possibility that earthquakes originating in the same active faults have a similar source process repeatedly.

For estimating strong ground motions in a deterministic approach, we need to have two kinds of source parameters, global and local ones .

Global Source Parameters

The global source parameters are total fault length and width, average slip and slip duration, rupture velocity and so on, which are to characterize the macroscopic pictures of given source faults. They are inferred , based on geological investigations of capable earthquake faults and seismological studies of source models.

Total fault lengths (L) of scenario earthquakes would be evaluated as one of the long-term seismic hazard evaluation. Some attempts have been making to estimate segmentation and grouping of active faults based on branching features of seismic surface ruptures (Matsuda, 1998). Such surveys give us **strike (ϕ)** and **slip type** of every segment consisting of the fault system. **Dip angle (δ)** is inferred from seismic reflection profile.

Fault width cannot be directly determined from the geological survey but mostly from source modeling for waveform simulations compared with observed records. Watanabe et al. (1998) made a plot (Fig. 3) to show the relation of fault width (W) vs. length (L), compiling 87 inland earthquakes from the source parameter catalog by Wells and Coppersmith (1994) and 5 large earthquakes by Abe (1990). The saturation of the width yields for events larger than M 6.8, corresponding the thickness of seismogenic zones. The seismogenic zones are infered from the depth-frequency distribution of small earthquakes (Ito, 1990). Recent study by Ito (1999) shows that The seismogenic zones seem to have upper cutoff depth as well as lower cutoff depth derived from the seimic-aseismic boundary in the mid-crust dependent on regions.

The **seismic moment** of the capable faults are estimated by the empirical relationship between the source areas and seismic source(A = LW), then average slips are automatically constrained by the seismic moment and source area (e.g. Somerville et al. 1999).

It is also very important source parameters where rupture start on the fault, to which directions, and where terminate. Rupture nucleate at the bottom of the seismogenic zones because of stress concentration in the seismic-aseismic boundary (Sibson, 1992). The starting point and propagation direction of rupture is identified from the patterns of surface traces from geographical investigations and theoretical modeling. Nakata et al. (1998) proposed a method to identify the direction of rupture propagation, the termination of rupture and in some cases, the epicenter location based on the branching features of active faults as shown in Fig. 4. Such ideas were examined by the dynamic theory of earthquake faulting. Kame and Yamashita (1998) numerically studied the effect of medium fracturing on the dynamic growth of earthquake rupture, suggesting that the faulting is needed to bend in the arresting of rupture or to make branching near its termination.

Local Source Parameters – Fault Heterogeneity or Roughness –

The slip and slip velocity have been found not to be uniform in the source areas, in particular for large earthquakes more than 7 as clarified from the waveform inversion of rupture process (Wald, 1996). We need to know slip and slip velocity distribution in the source area as well as the average slip to estimate strong ground motions. We call here such source parameters local source parameters that express fault heterogeneity or roughness. So far slip models have been derived from longer period ground motions using the waveform inversion. Direct application of such long-period source models to strong ground motion estimation is not always available because higher ground motions than 1 Hz cannot be generated. Nevertheless, we found that the asperity models derived from the heterogeneous slip distribution using the waveform inversion of longer-period ground-motion recordings are available for estimating broad-band ground motions of engineering interest (e.g. Kamae and Irikura, 1998).

Somerville et al. (1999) analyzed the characteristics of slip models of totally fifteen crustal earthquakes ranging from about 6 to 7 in moment magnitude(Mw) for use in the prediction of strong ground motion. They used two approaches, deterministic and stochastic, in characterizing the slip models.

First they define **fault asperities** in a deterministic manner to quantify the properties of heterogeneous slip models. The asperities are areas on the fault rupture surface that have large slip relative to the average slip on the fault. An asperity is defined to enclose fault elements whose slip is 1.5 or more times larger than the average slip in the fault (in detail refer to Somerville et al.,1999). The number of asperities in the slip models of those events is 2.6 on average. The slip contrast, the average slip on the asperities over average slip is about 2. The combined area of asperities on average occupies about 22 % of the total rupture area.

Total rupture area (A), combined area of asperities (Aa), and area of largest asperity (Am) scale in a self-similar manner with increasing seismic moment.

$$A(km^2) = 2.23 \times 10^{-15} \times Mo^{2/3}(dyne \cdot cm) \quad (1)$$
$$Aa(km^2) = 5.00 \times 10^{-16} \times Mo^{2/3}(dyne \cdot cm) \quad (2)$$
$$Am(km^2) = 3.64 \times 10^{-16} \times Mo^{2/3}(dyne \cdot cm) \quad (3)$$

Other parameters such as average asperity slip, hypocentral distance to closest asperities, slip duration also scale

with seismic moment in the self-similar way.
Second, they used the stochastic approach to quantify the heterogeneity of slip on the fault surface by its two-dimensional Fourier transform (the wavenumber spectrum). They derived a model for **the wavenumber spectrum of spatial slip distribution** on the fault which falls off as the inverse of the k-squared at high wavenumbers, consistent with the model of Herrero and Barnard(1994). The k-squared model is consistent with the fractal model of Frankel (1991) when the fractal dimension is 2, resulting in a kinematic source model with the omega-squared model (Aki, 1967).
The validity and applicability of strong ground prediction and the relation between strong ground motions and structure damage should be examined in comparison with the observed records and actual damage during the 1995 Hyogo-ken Nanbu (Kobe) earthquake. We find that the source model with three asperities for the 1995 Hyogo-ken Nanbu (Kobe) earthquake by Kamae and Irikura (1998) also follows the k-squared model.

HYPOTHETICAL EARTHQUAKES

We take up Osaka, one of the biggest cities in Japan, to estimate strong ground motion for hypothetical large earthquakes representing a potentially serious seismic damage. We select four active faults as hypothetical earthquakes to estimate design ground motions in the Osaka Prefecture area, the Uemachi Fault, the Ikoma Fault, the Arima-Takatsuki Tectonic Line, and the Median Tectonic Line as shown in Fig. 5. The criteria for precaution faults are set as follows: (1) active faults that are judged to be high certainties of existence from geological survey and to have high degrees of activity from slip rate; and (2) that have possibilities of causing very severe damages to subject buildings and facilities, because they are expected to seismic magnitudes large enough and fault distance short enough.
The basic information about the location of the faults and the global source parameters such as length (L), strike (ϕ_S), and slip type of each fault was referred to "Active Faults of Japan, revised edition " by Research group of Active Faults in Japan (1991). Dip angle δ are estimated by reflection profiling, for example cross-sections across the Uemachi Fault by reflection method indicates 60 degrees for reverse faults. Fault width W was estimated from the relationship $W = Zc/\sin\delta$, where Zc is the cutoff depth from the aftershock distribution of the 1995 Hyogo-ken Nanbu earthquake and microearthquake distribution in this region.
The local source parameters such as the areas and stress drops of the asperities are obtained following the self-similar relations (1), (2), and (3). For example, the fault model of the Uemachi Fault earthquake is shown in Fig. 6. The location of the asperities are inferred from the fault geometry. For those parameters we should consider certain variances and evaluate their influences on ground motion prediction although not describe here.

Prediction of Strong Ground Motion at Representative Points in Osaka

Strong ground motions are evaluated at representative points in Osaka from the Arima-Takatsuki tectonic line, the Uemachi fault, the Ikoma fault and the Median Tectonic line earthquakes (Irikura, 1998). The estimation is done by the hybrid Green's function method. Long-period ground motions are calculated by the three-dimensional finite difference method (Pitarka et al. 1998) considering realistic 3-D geological configurations (Kagawa et al. 1993). Short-period ground motions are simulated by the Boore method (1983) considering empirical site effects (Tsurugi et al., 1997). Then both short and long period motions are superposed as a hybrid Green's function., ground motions from small earthquakes at the case-study points.

Examples of ground motions estimated at sites on different grounds

Examples of ground motions at the case-study points from hypothetical earthquakes are shown in a), b), c), and d) of Fig. 7. Those points are on the surface of grounds with different soil conditions.
a) Bedrock in the northern part of Osaka from the Arima-Takatsuki tectonic line earthquake: Ground motions estimated at the Minoo River dam (a in Fig. 7) on bedrock from the Arima-Takatsuki tectonic line earthquake are shown in a) of Fig. 8. This point is at the shortest distance of 3 km from the fault. Estimated values are: maximum acceleration 341 gals, maximum velocity 45 cm/s and maximum displacement 9.2 cm. It is characteristic of the rock ground motions that the short-period component predominates without later phases such as surface waves.
b) Pleistocene ground in the northern part of Osaka from the Arima-Takatsuki tectonic line earthquake: Ground motions estimated at Osaka monorail P365 (b in Fig. 7) on Pleistocene ground from the Arima-Takatsuki tectonic line earthquake are shown in b) of Fig. 8. It is at the shortest distance of about 4 km from the fault. Duration of waveforms is relatively short compared with that at alluvium sites. Predominant periods are about 0.6 sec but change dependent on fault distance and site conditions. The amplitudes even at the longer periods from 1.0 sec to 2.0 sec are larger than those at the bedrock in a).

c) Alluvium ground in the eastern part of Osaka from the Ikoma fault earthquake: Ground motions at Osaka central loop line (c in Fig. 7) on alluvium ground from are shown in c) of Fig. 8. The shortest distance to the fault is about 6.0 km. It is known that this point has relatively thick sedimentation of alluvium, several tens meter and the bedrock depth under this point is large, more than 1 km. Consequently, ground motions with the periods of about 0.6 sec and 2.0 sec predominate. Later phases are not strongly excited, but their duration is longer, compared with the waveforms of a) and b).
d) Alluvium ground in the western part of Osaka from the Uemachi fault earthquake: Ground motion at the Kizu River (d in Fig. 7) on alluvium ground from the Uemachi fault earthquake are shown in d) of Fig. 8. Estimated waveforms are characteristic of distinctive later phases, so-called "after-shake" phenomena, arriving with the delay time of about 20 seconds after direct waves. These after-shake waves are presumed to be ground motion diffracted at the edges of sedimentary basin near the Ikoma fault.

CONCLUSION

We summarized the procedure for predicting strong ground motions from future earthquakes caused by inland active faults as a recipe. The Green's functions in broad frequency band are calculated in hybrid scheme, deterministic and stochastic approaches, taking into account realistic 3-D structure. The source characterization for the future earthquakes are made by the statistical analysis of the source inversion using strong motion and teleseismic data. Referring to Somerville et al. (1998) we find that the combined area of asperities as well as total rupture area follows the self-similar scaling and the wave-number spectra for the final slip model fit to the k-squared model at high-wavenumbers. The source model composed of several asperities for the 1995 Hyogo-ken Nanbu earthquake coincide with the source characterization obtained above.
Then, we attempted to simulate strong ground motions for hypothetical large earthquakes in the Osaka metropolitan area. Four active faults surrounding the Osaka basin are selected as scenario earthquakes based on geological and seismological surveys. The near-fault motions synthesized for soil sites are characterized by large acceleration responses more than 2,000 gals.
Estimation of strong ground motion at representative points in Osaka prefecture clarify the following. (i) In the waveforms of the bedrock, short-period components predominate and later phases after direct waves are not observed. (ii) In the waveforms of the Pleistocene ground, short-period components predominate, but ground motion with the periods of 1.0 sec - 2.0 sec are greater than those in the bedrock. (iii) In the alluvium ground, the "after-shake" phenomena, characteristic of the Osaka basin, are reproduced. (iv) As a result of investigating acceleration response spectra depending on ground type, they were found to be nearly equal to or smaller than the seismic design spectra for bridge structures regulated in 1996.
This study was partially supported by a grant-in-Aid for Scientific Research, Number 08248111, from the Ministry of Education, Science, Sports, and Culture.

REFERENCES

Abe, K.. (1990), "Seismological aspects of Luzon, Philippines earthquake of July 16, 1990", *Bull. Earthq. Res. Inst.*, 65, pp851-874 (in Japanese)
Aki, K. (1967), "Scaling law of seismic spectrum", *J. Geophys. Res.*, 72, pp217-231.
Boore, D. M. (1983), "Stochastic simulation of high-frequency ground motions based on seismological models of the radiated spectra", *Bull. Seism. Soc. Am.*, 73, pp1865-1894.
Bouchon, M., H. Sekiguchi, K. Irikura, and T. Iwata (1998), "Some characteristics of the stress field of the 1995 Hyogo-ken Nanbu (Kobe) earthquake", *J. Geophys. Res.*, 103, pp24,271-24,282.
Frankel, A. (1991), High-frequency spectral fall-off of earthquakes, fractal dimension of complex rupture, b value, and the scaling strength on Fault", *J. Geophys. Res.*, 96, pp6,291-6,302.
Herrero, A. and P. Bernard (1994), "A kinematic self-similar rupture process for earthquakes", *Bull. Seism. Soc. Am.*, 84, pp1216-1228 .
Irikura, K. (1986), "Prediction of strong acceleration motion using empirical Green's function", *Proc. 7th Japan Earthq. Eng. Symp.*, pp151-156.
Irikura, K. (1998), "Prediction of strong motions from future earthquakes in the Osaka basin", *Proc 2nd Inter. Symp. on Effects of Surface Geology on Seismic Motion*, 1, pp171-188.
Irikura and Kamae (1999), "Strong ground motions during the 1948 Fukui earthquake", *Zisin (J. Seism. Soc. Japan)*, 52, pp129-150 (in Japanese).
Ito, K. (1990), "Regional variations of the cutoff depth of seismicity in the crust and their relation to heat flow and large inland-earthquakes", *J. Phys. Earth.*, 38, pp223-250.
Ito, K. (1999), "Seismogenic layer, reflective lower crust, surface heat flow and large inland-earthquakes",

Tectonophysics, 306, pp423-433.
Kagawa, T., S. Sawada, Y. Iwasaki, and A. Nanso (1993), "Modeling of deep sedimentary structure beneath the Osaka basin". *Proc. 22th JSCE Earthquake Engineering Symposium*, pp199-202 (in Japanese).
Kame, N. and T. Yamashita (1998), "Why are the numeber of small earthquakes larger than that of large earthquakes ? –spontaneous arresting of earthquake rupture –", *KAGAKU*. 68: 702-709 (in Japanese).
Kamae, K. and K. Irikura (1998), "Source model of the 1995 Hyogo-ken Nanbu earthquake and simulation of near-source ground motion", *Bull. Seism. Soc. Am.* , 88, pp400-412.
Kamae, K. , K. Irikura and A. Pitarka (1998), "A technique for simulating strong ground motion using hybrid Green's function", *Bull. Seism. Soc. Am.* , 88, pp 357-367.
Matsuda, T. (1998), "Present state of long-term prediction of earthquakes based on active fault data in Japan, *Zisin (J. Seism. Soc. Japan)*, 50, pp23-34 (in Japanese).
Nakata, T., K. Shimazaki, Y. Suzuki, and E. Tsukuda (1998), "Fault branching and directivity of rupture propagation", *Journal of Geography*, 107, pp512-528 (in Japanese).
Pitarka, A. and Kojiro Irikura (1996), "Modeling 3D surface topography by finite-difference method: Kobe-JMA station site, Japan, case study", *Geophys. Res. Lett.*, 23, pp2729-2732.
Pitarka, A., K. Irikura and T. Iwata (1997), "Modeling of ground motion in Higashinada (Kobe) area for an aftershock of the January 17, 1995, Hyoto-ken Nanbu, Japan, earthquake", *Geophysical Journal International*, 131, pp231-239.
Pitarka, A., K. Irikura, T. Iwata, and H. Sekiguchi (1998), "Three-dimensional simulation of the near-fault ground motion for the 1995 Hyogo-ken Nanbu (Kobe), Japan, earthquake", *Bull. Seism. Soc. Am.* , 88, pp428-440.
Research Group of Active Faults in Japan (1991), "Active Faults in Japan revised edition", *University of Tokyo Press* (in Japanese).
Sekiguchi, H., K. Irikura, T. Iwata, Y. Kakehi, and M. Hoshiba (1996), "Minute locating of faulting beneath Kobe and the waveform inversion of the source process during the Hyogo-ken Nanbu, Japan, earthquake using strong ground motion records", *J. Physics of the Earth*. 44, pp473-488.
Sibson, R. H. (1992), "Implications of fault-valve behaviour for rupture nucleation and recurrence", *Tectonophysics*, 211, pp283-293.
Somerville, P., K. Irikura, R. Graves, S. Sawada, D.Wald, N. Abrahamson, Y. Iwasaki, T. Kagawa, N. Smith, and A. Kowada (1998), "Characterizing earthquake slip models for the prediction of strong ground motion", *Seismological Research Letters*, 70, pp59-80.
Tsurugi, M., M. Tai, K. Irikura, and A. Kowada (1997), "Estimation of empirical site amplification effects using observed records", *Zisin (J. Seism. Soc. Japan)*, 50, 215-228 (in Japanese).
Wald, D. J. (1996), "Slip history of the 1995 Kobe, Japan, earthquake determined from strong motion, teleseismic, and geodetic data", J. Phys. Earth, 44, pp489-503.
Watanabe, M., T. Sato, and K. Dan (1998), "Scaling relations of fault parameters for inland earthquakes", *Proc. 10th Japan Earth. Eng. Symp.*, 1, pp583-588.
Wells, D. L. and K. L. Coppersmith, 1994, New empirical relationships among magnitude, rupture width, rupture area, and surface displacement", *Bull. Seism. Soc. Am.* , 84, pp974-1002.

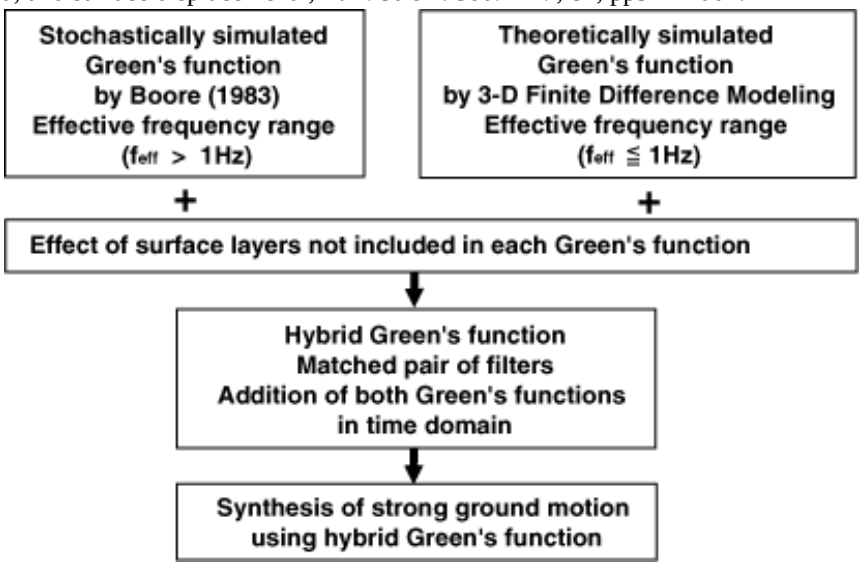

Figure 1: Flow chart of simulating strong ground motions using the hybrid Green's function method.

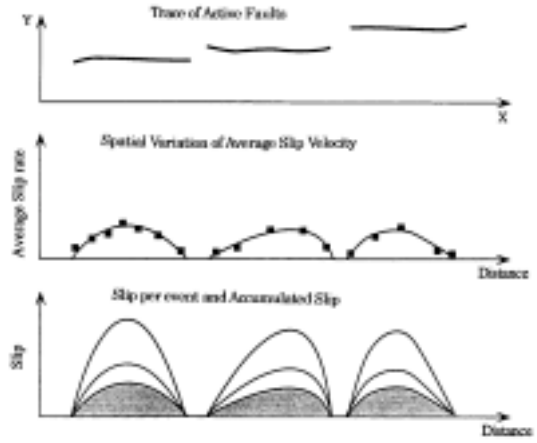

Figure 2. Spatial distribution of fault traces, average slip velocity, and accumulated slip.

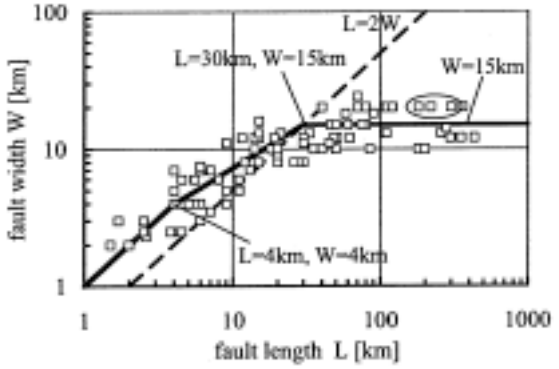

Figure 3. Relation of fault width versus fault length for inland crustal earthquakes.

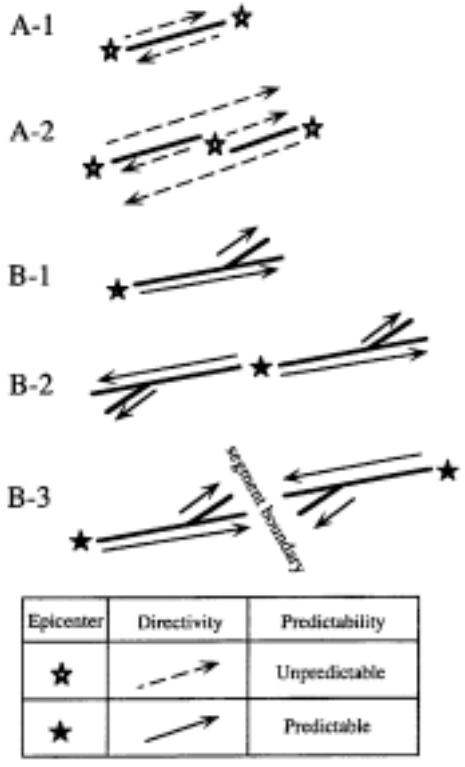

Figure 4. Illustrative models of fault branching and rupture propagation (After Nakata et al., 1998)

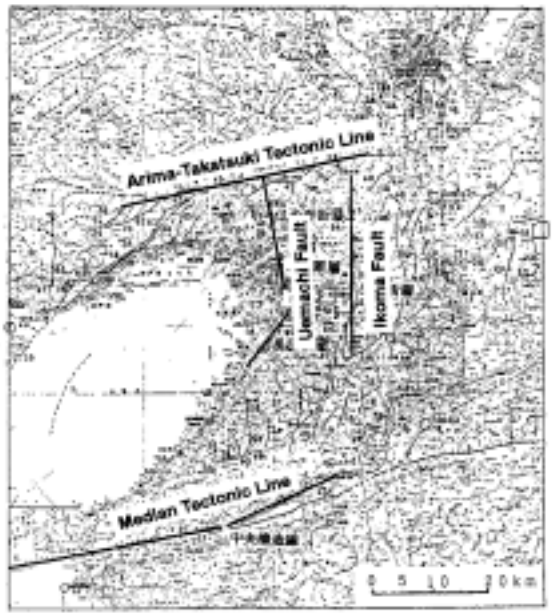

Figure 5. Locations of four active faults considered as hypothetical earthquakes in the Osaka Prefecture area, the Uemachi Fault, the Ikoma Fault, the Arima-Takatsuki Tectonic Line, and the Median Tectonic Line.

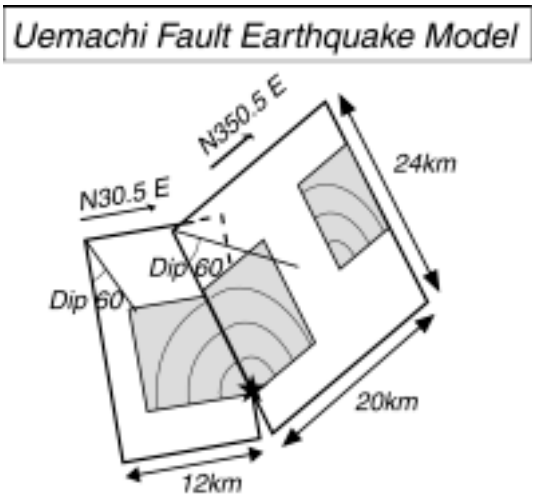

Figure 6. Source model of the Uemachi Fault earthquake.

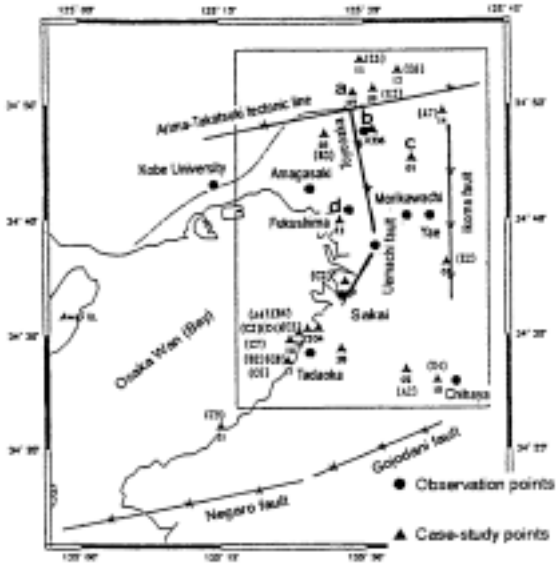

Figure 7. Locations of hypothetical earthquake faults and 30 representative points for estimating ground motions. Ground motions at a, b, c, and d are shown in Figure 8.

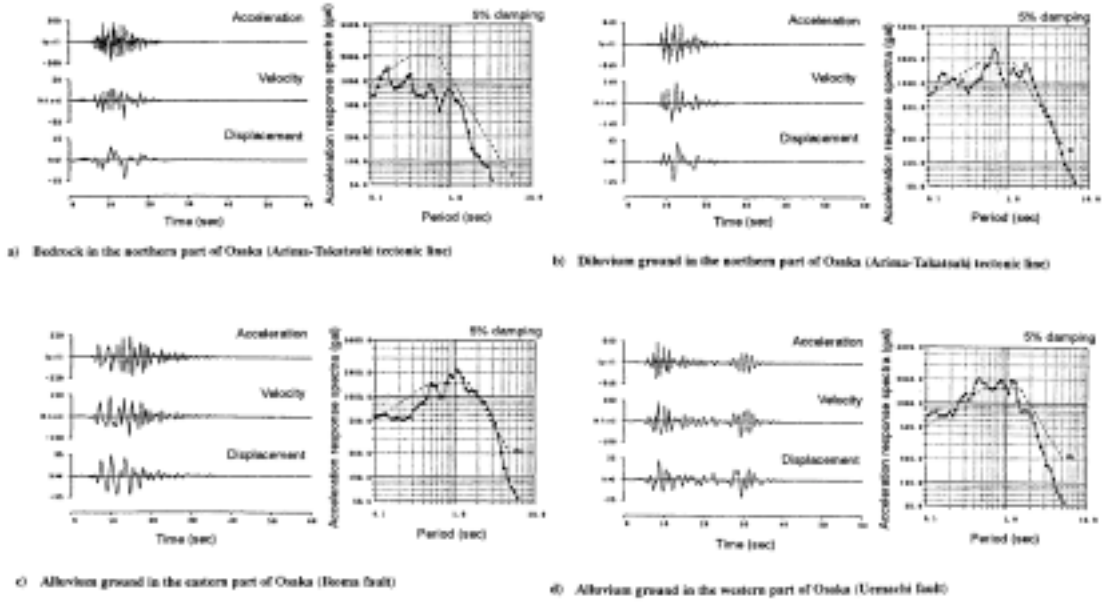

Figure 8. Example of estimated strong ground motions (acceleration, velocity, displacement, and acceleration response spectrum) from hypothetical earthquakes. Estimated acceleration response spectrum is compared with design spectrum dependent on ground conditions.